Lattice Fringe Fingerprinting in Two Dimensions with Database Support

P. Moeck[*,Ω,♦], B. Seipel[*,Ω], R. Bjorge[*] and P. Fraundorf[**]

[*]Department of Physics, Portland State University, P.O. Box 751, Portland, OR 97207-0751, U.S.A.
[Ω] Oregon Nanoscience and Microtechnologies Institute, http://www.onami.us
[♦] Advisory Board of the Crystallography Open Database, http://crystallography.net
[**]Department of Physics and Astronomy & Center for Molecular Electronics, University of Missouri at St. Louis, MO 53121, U.S.A.

Abstract

A brief introduction to lattice fringe fingerprinting in two dimensions (2D) with database support is given. The method is employed for the identification of the crystal phase of a small ensemble of nanocrystals. The enhanced viability of this method in aberration-corrected transmission electron microscopes (TEMs) and scanning TEMs (STEMs) is also illustrated.

Keywords: transmission electron microscopy, open crystallographic databases, nanocrystals

1 Introduction

It is well known that the physical and chemical properties of nanocrystals are determined by both their structures (i.e. 3D long-range ordered atomic arrangements) and morphologies (i.e. extended 2D discontinuities of the atomic arrangement). Structural prototypes, lattice constants, and morphologies of nanocrystals are frequently dependent on the size of the crystals in the nanometer range. Added to this size dependency of the lowest thermo-dynamical potential of a structure, there is in the nanoparticle regime a strong tendency towards metastability and spatially inhomogeneous non-stoichiometry.

Moreover, many nanocrystals possess structural defects in three, two, and one dimension(s) as well as point defects in excess of their thermodynamical equilibrium levels. The presences of these structural defects are dependent on the particulars of the nanocrystal synthesis and processing procedures and significantly affect the properties of the nanoparticles.

In short, a whole new "crystallographic world" is waiting to be discovered in the nanocrystal realm. Eventually, core models of text book crystallography such as ideal crystals being represented by the infinite translation of unit cells, may have to be modified on the basis of such discoveries. To aid such discoveries, we briefly describe here the novel method of fringe fingerprinting in 2D with database support. Theoretical fringe fingerprint plots of the titania polymorphs rutile, anatase, and brookite are used to illustrate the phase identification of a small ensemble of "quasi-unknown" nanocrystals. The enhanced viability of our method in aberration-corrected TEMs and STEMs is also briefly illustrated.

2 Description of the method

Fringe fingerprinting in 2D was recently proposed by the authors of this paper [1,2]. Fringe fingerprint plots (which may be called angular covariance plots alternatively) represent, in their most basic form, plots of (visible) interfringe angles of crossed lattice fringes versus the respective reciprocal lattice spacings of these (visible) fringes. The criterion for a fringe being visible is that its spatial frequency is reliably transferred to the high-resolution phase-contrast TEM or atomic resolution STEM image. Such a reliable transfer is achieved up to the point resolution (point-to-point, also called Scherzer resolution in the phase-contrast mode) of a non-aberration corrected microscope. Apertures are typically employed to remove spatial frequencies beyond this limit.

Figures 1 - 3 show theoretical fringe-fingerprint plots (in the kinematical limit) for ensembles of nanocrystals of the three titania polymorphs rutile, anatase, and brookite. While there are two data points in such plots for cross-fringes with different spacings, the crossing of two symmetrically related fringes (which possess by symmetry the same spacing) results in just one data point, see insets in Fig. 1.

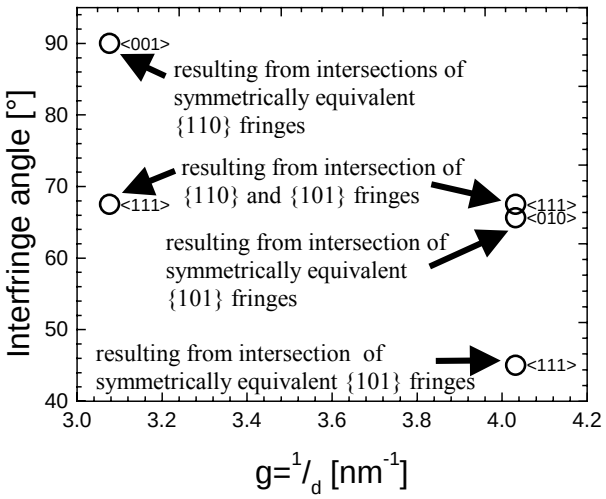

Figure 1: Basic theoretical fringe fingerprint plot for rutile, space group $P4_2/mnm$, a = 0.459 nm, c = 0.296 nm, microscope point resolution 0.24 nm (as obtainable with state-of-the-art analytical TEMs).

Projection effects, i.e. fringe spacings appearing shrunken by a factor of cos γ in the direction perpendicular to the tilt axis, will be larger the smaller the nanocrystals are. This is because fringe crossings/zone axes will be visible over a wider angular range (γ) for smaller nanocrystals, as can be calculated from the equations given in ref. [1]. Similarly, foreshortening projection effects of interfringe angles can be readily corrected for [3].

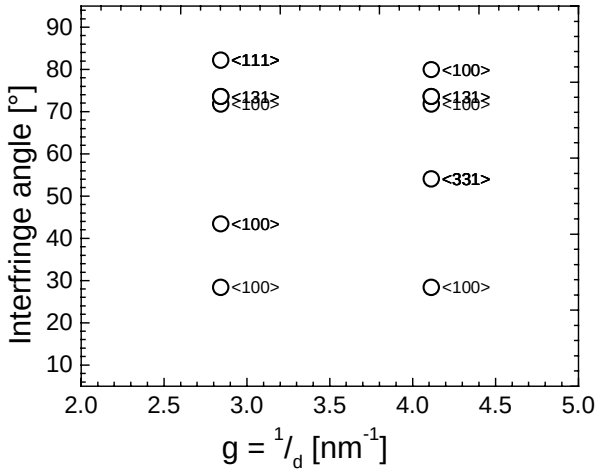

Figure 2: Basic theoretical fringe fingerprint plot for anatase, space group $I4_1/amd$, a = 0.378 nm, c = 0.951 nm, microscope point resolution 0.24 nm.

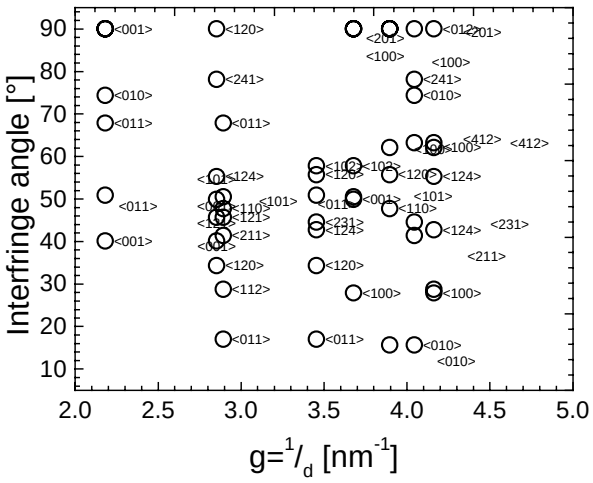

Figure 3: Basic theoretical fringe fingerprint plot for brookite, space group Pbca, a = 0.918 nm, b = 0.546 nm, c = 0.514 nm, microscope point resolution 0.24 nm.

The utility of basic theoretical fringe-fingerprint plots, Figs. 1 - 3, and their more elaborate cousins that are mentioned in the final section of this paper, is founded in them being a rather specific characteristic for an ensemble of nanocrystals against which experimental data from high resolution TEM or atomic resolution STEM images can be directly compared for the identification of unknown nanocrystal phases.

Figure 4 shows, for example, an experimental fringe fingerprint plot from an ensemble of nanocrystals that were intended to be used in solar cells [4]. The comparison between the experimental fringe fingerprint plot, Fig. 4, with the theoretical fringe fingerprint plots of the titania phases rutile, Fig. 1, anatase, Fig. 2, and brookite, Fig. 3, indicates that these nanocrystals possess the rutile phase. Comparison of Fig. 4 to Fig. 1 indicates that all nanocrystals were oriented close to <111>.

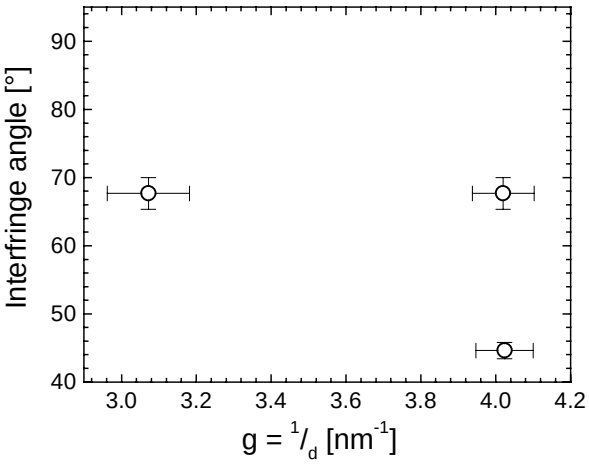

Figure 4: Experimental fringe fingerprint plot of an ensemble of "quasi-unknown" nanocrystals (expected to be anatase [4]). This plot arises from 5 individual nanocrystals of which high-resolution phase contrast TEM images were recorded in an analytical FEI Tecnai G^2 F20 ST TEM/STEM. Due to the preliminary nature of this investigation, the relative errors in the spatial frequencies are several percent. Possible differences in the lattice constants of the nanocrystals from those of the corresponding bulk materials are, therefore, to be neglected. (Energy dispersive X-ray spectroscopy from the same sample in the TEM showed only peaks for Ti, but not for Sn. The latter would be an indication of the possible presence of SnO_2, which is in the cassiterite modification isomorphic to rutile and possesses, therefore, a similar fringe fingerprint plot. Note that a continuous SnO_2 layer of several μm thickness was part of the sample [4] before the scraping off of the nanocrystals for the TEM analyses, but is unlikely to have been mistaken for the nanocrystals.)

3 Enhanced viability of the method with improved point resolution of electron microscopes

Just as with all other applications of image-based nano-crystallography [1,2,5], lattice fringe fingerprinting in 2D will be more viable as more and more fringes become visible in high-resolution phase-contrast TEM or atomic resolution STEM images, Table 1.

When we take, in a purely phenomenological manner, the number of data points in fringe fingerprint plots of rutile, (Fig. 1 and the second column of Table 1), as a measure of the viability of fringe fingerprinting in 2D, there is a strongly super-linear increase in viability [5] with improvements of the point resolution of electron microscopes. Point resolutions of approximately 0.1 nm are achievable on a

routine basis in the current generation of lens-aberration corrected TEMs and STEMs [6].

Point resolution [nm] of microscopes	Number of data points in fringe fingerprint plots of rutile
0.24	5 (from 3 zone axes, see also Fig. 1)
0.19	40 (from 9 zone axes)
0.14	Approximately 130
0.09	Approximately 1000 (as obtainable by means of aberration-corrected objective or condenser lenses [6])

Table 1: Number of data points in (kinematical limit) fringe fingerprint plots of rutile as a function of the point resolution of electron microscopes.

4 Comparison of the method to electron powder diffractogram fingerprinting

Figures 5 - 7 show theoretical powder electron diffractograms of rutile, anatase, and brookite normalized to 100 % of the largest intensity peak and up to the spatial frequency 4.17 nm^{-1} (background free and crystal size independent calculations using the program described in ref. [7]). This spatial frequency corresponds to the microscope point resolution of 0.24 nm we chose to present Figs. 1 to 3. The abscissa information in all six figures is, therefore, the same. There is also a correspondence between Table 1 and Table 2, whereby the latter shows how the number of peaks in powder electron diffractograms of rutile increases as a function of spatial frequency.

Spatial frequency [nm^{-1}]	Number of peaks (rings) in powder electron diffractograms of rutile
4.17	2
5.26	5
7.14	10
11.11	32

Table 2: Number of peaks (rings) in powder electron diffractograms of rutile as a function of spatial frequency.

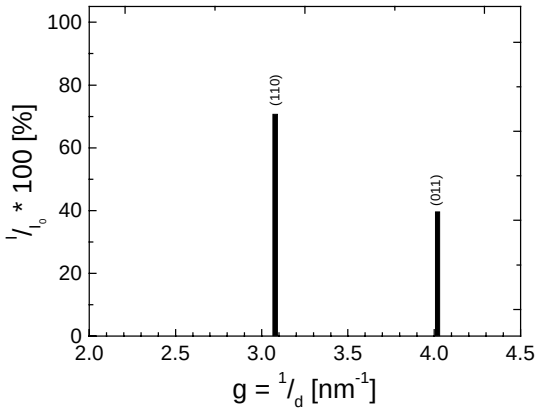

Figure 5: Calculated powder electron diffractogram for rutile.

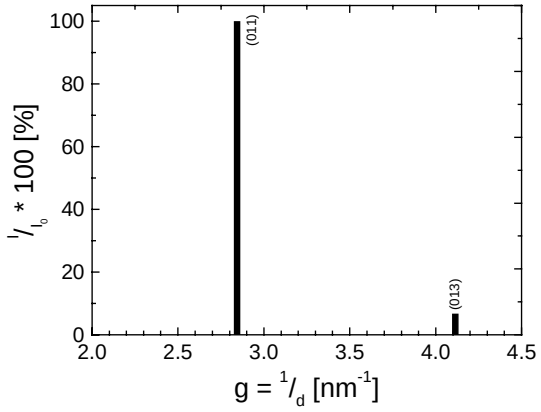

Figure 6: Calculated powder electron diffractogram for anatase.

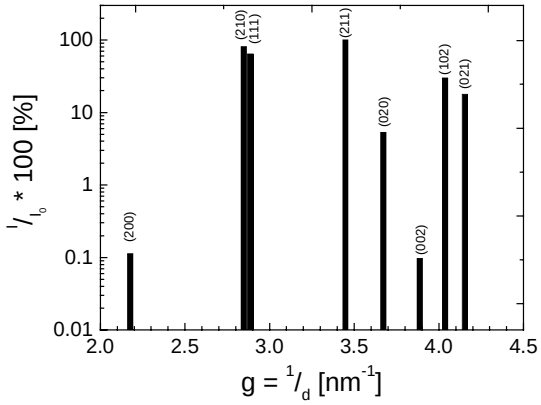

Figure 7: Calculated powder electron diffractogram for brookite. Note that the abscissa is given in a logarithmic scale.

Obviously, the characteristic information that can be employed to identify unknown crystal phases increases much more rapidly with improved resolution in fringe fingerprint plots, Table 1, than in electron powder diffractograms, Table 2. In addition, lattice fringe fingerprint plots contain for the same spatial frequency more crystallographic information. Image-based nanocrystal-lographic analyses in aberration-corrected microscopes can, therefore, complement their parallel-beam diffraction-based nanocrystallographic counterparts [8].

Note that classical crystallometry (morphological crystallography, also called optical goniometry) [9] enabled two comprehensive databases with about 8000 entries. The organizing principle of both databases [10,11] is interfacial angles, and they were used for decades to identify unknown crystals from their interfacial angles alone [9]. Because the dominating crystal forms are typically the low indexed net planes, which possess the largest spacings in direct space, it is precisely those angles that are also reproduced in lattice fringe fingerprint plots.

Fringe fingerprint plots, Figs. 1 - 4, thus, combine information that is contained in powder electron diffractograms (spatial frequency plots), Figs. 5 - 7, and their related spatial frequency databases [12], as well as in the

above mentioned crystallometry (interfacial angles) databases [10,11]. Fringe fingerprint plots are, therefore, crystallographically more characteristic "finger prints" than those that are derived from either of these two types of databases [10-12]. As with any kind of "finger print" one needs the support of a comprehensive database to identify an unknown.

In 2005, the "Nanocrystallography Group" at Portland State University started the development of a freely accessible on-line database that supports fringe fingerprinting in (both) 2D (and 3D employing tilt protocols [1]). This database is called "Nano-Crystallography Database" (NCD) [13] and relies partly on data from the freely accessible on-line "Crystallography Open Database" [14].

The entries in both databases are in the "Crystallographic Information File" [15] format standard. (In total reports on more than 31,000 full structure determinations are currently available for free at these web sites [13,14].) At the NCD web site, we provide three-dimensional visualizations and their respective 2D projections as well as theoretical fringe fingerprint plots for several thousand compounds and elements.

With support from our NCD, fringe fingerprinting in 2D may become one of the realizations of Boldyrew's and Doliwo-Dobrowolsky's 70 years old prophecy [16]: ***"In the further development of crystallography one will either adopt one of the goniometric methods of determining crystals or develop eventually a new one which, as far as this is possible, combines the advantages of all of the prior methods and avoids their disadvantages."***

5 Outlook on further developments of the method

More elaborate theoretical fringe fingerprint plots than those given in Figs. 1 - 3 may contain (as part of a two-dimensional histogram, i.e. a three-dimensional plot) the probability of seeing crossed fringes in an ensemble of randomly oriented nanocrystals. Such probabilities can be calculated from our kinematical theory of lattice fringe visibility [1]. Another type of more elaborate fringe fingerprint plots may contain, encoded as (three-dimensional) data point density, both the probabilities of detecting crossed fringes and the angular and spatial frequency ranges over which the fringe crossings/zone axes are visible, possibly both also as a function of nanocrystal thickness [1]. Such "advanced lattice fringe fingerprint" plots will obviously be much more characteristic of the phase of nanocrystals than electron diffractograms, Figs. 5 – 7, even for non-aberration corrected TEMs and STEMs.

6 Conclusions

Lattice fringe fingerprinting of nanocrystals in two dimensions with database support has been demonstrated and briefly compared to electron powder diffractometry. The crystal phase of an "unexpected", i.e. "quasi-unknown" nano-crystal ensemble has been identified as rutile.

7 Acknowledgments

This research was supported by an award from Research Corporation. The NorthWest Academic Computing Consortium and faculty enhancement/development awards by Portland State University (PSU) provided additional support. Prof. Rolf Koenenkamp (of PSU) is thanked for the high-resolution phase-contrast TEM images we "fringe fingerprinted" (and the associated energy dispersive X-ray spectroscopy results).

References

[1] P. Fraundorf, W. Qin, P. Moeck, and E. Mandell, *J. Appl. Phys*. **98**, 114308, 2005; arXiv:cond-mat/0212281 v2.

[2] P. Moeck, O. Čertík, B. Seipel, R. Groebner, L. Noice, G. Upreti, P. Fraundorf, R. Erni, N. D. Browning, A. Kiesow, and J.-P. Jolivet, *Two- and Three-Dimensional Methods for Inspection and Metrology III*, edited by K.G. Harding, *Proc. of SPIE*, Vol. **6000**, 60000M-1, 2005.

[3] J.D.H. Donnay and W.A. O'Brien, Ind. Engin. Chem. Anal. Ed., **17**, 593,1945.

[4] R. Könenkamp, P. Hoyer, and A. Wahl, J. Appl. Phys. **79**, 7029, 2005.

[5] P. Moeck, W. Qin, and P. Fraundorf, *Nonlinear Analysis* **63**, e1323, 2005.

[6] S.J. Pennycook, M. Varela, C.J.D. Hetherington, and A.I. Kirkland, MRS Bulletin **31**, 36, 2006.

[7] W.T. Pennington, *J. Appl. Cryst*. **32**, 1028, 1999.

[8] J.M. Zuo, "Electron nanocrystallography", Chapter 18 in: Handbook of Microscopy for Nanotechnology, Eds. N. Yao and Z.L. Wang, Kluwer Academic Publ., Boston, Dordrecht, New York, London, 2005.

[9] P. Terpstra and L.W. Codd, Crystallometry**,** Academic Press, New York, 1961.

[10] M.W. Porter and R.C. Spiller, *The Barker Index of Crystals*, Vol. I and II, W. Heffer and Sons, Cambridge, 1951 and 1956; M.W. Porter and L.W. Codd, *The Barker Index of Crystals***,** Vol. III, W. Heffer and Sons, Cambridge, 1964.

[11] A.K. Boldyrew and W.W. Doliwo-Dobrowolsky, *Bestimmungstabellen für Kristalle*, Vol. I, Part 1 & Part 2, Труды Центрального научно-исследовательского Геолого-разведочного Института, Leningrad and Moscow, 1937 and 1939.

[12] J. Faber, T. Fawcett, and R. Goehner, *Microsc. Microanal*. **11**(Suppl. 2), 778, 2005.

[13] http://nanocrystallography.research.pdx.edu.

[14] http://crystallography.net.

[15] I.D. Brown and B. McMahon, *Acta Cryst.* B**58**, 317, 2002.

[16] A.K. Boldyrew and W.W. Doliwo-Dobrowolsky, *Zeits. Krist.* **A 93**, 321,1936.